National Institute of Information and Communications Technology
Time-Space Standards Group
4-2-1 Nukui-Kita, Konaganei, Tokyo, 184-8795, Japan

Attached is the preliminary results of our evaluation of atomic fountain primary frequency standard NICT-CsF1 performed four times over the 15 day period of MJD 54014 to 54029, the 10 days period of MJD 54029-54039, the 10 days period of MJD 54039-54049, the 15 days period of MJD 54079-54094. The detail of the evaluation is discussed in this report.

Motohiro Kumagai
Masatoshi Kajita
Hiroyuki Ito
Mizuhiko Hosokawa

11 pages

1. Evaluations of primary frequency standard NICT-CsF1

Interval	MJD 54014 UTC 0:00 - 54029 UTC 0:00 (15days)
Cycle duty	98.0%
Frequency difference	Y(NICT-CsF1 – UTC(NICT)) = $+0.2 \cdot 10^{-15}$
Type B uncertainty u_B	$2.5 \cdot 10^{-15}$
Type A uncertainty u_A	$1.0 \cdot 10^{-15}$
Link to clock $u_{link/lab}$	$0.3 \cdot 10^{-15}$
Link to clock $u_{link/TAI}$	$0.9 \cdot 10^{-15}$
Combined uncertainty	$2.9 \cdot 10^{-15}$

Interval	MJD 54029 UTC 0:00 - 54039 UTC 0:00 (10days)
Cycle duty	99.0%
Frequency difference	Y(NICT-CsF1 – UTC(NICT)) = $+1.9 \cdot 10^{-15}$
Type B uncertainty u_B	$2.8 \cdot 10^{-15}$
Type A uncertainty u_A	$1.0 \cdot 10^{-15}$
Link to clock $u_{link/lab}$	$0.3 \cdot 10^{-15}$
Link to clock $u_{link/TAI}$	$1.2 \cdot 10^{-15}$
Combined uncertainty	$3.2 \cdot 10^{-15}$

Interval	MJD 54039 UTC 0:00 - 54049 UTC 0:00 (10days)
Cycle duty	98.5%
Frequency difference	Y(NICT-CsF1 – UTC(NICT)) = $-1.4 \cdot 10^{-15}$
Type B uncertainty u_B	$1.6 \cdot 10^{-15}$
Type A uncertainty u_A	$1.0 \cdot 10^{-15}$
Link to clock $u_{link/lab}$	$0.3 \cdot 10^{-15}$
Link to clock $u_{link/TAI}$	$1.2 \cdot 10^{-15}$
Combined uncertainty	$2.3 \cdot 10^{-15}$

Interval	MJD 54079 UTC 0:00 - 54094 UTC 0:00 (15days)

Cycle duty	99.0%
Frequency difference	Y(NICT-CsF1 – UTC(NICT)) = $+3.6 \cdot 10^{-15}$
Type B uncertainty u_B	$1.9 \cdot 10^{-15}$
Type A uncertainty u_A	$1.0 \cdot 10^{-15}$
Link to clock $u_{link/lab}$	$0.3 \cdot 10^{-15}$
Link to clock $u_{link/TAI}$	$0.9 \cdot 10^{-15}$
Combined uncertainty	$2.3 \cdot 10^{-15}$

A brief description of the various biases and uncertainties is presented in the following sections of this report. A detailed description of NICT-CsF1 and the uncertainty evaluation is given in [1]

2. Systematic (Type B) Uncertainty of NICT-CsF1

A. Second-order Zeeman shift

The correction for the second-order Zeeman shift is calculated by monitoring the (F=4, m_F =1) – (F=3, m_F =1) transition with linear dependence on the magnetic field B. Denoting a frequency separation between the clock transition and the (F=4, m_F =1) – (F=3, m_F =1) transition as $\nu_{1\text{-}1}$, the second-order Zeeman shift is given by

$$\frac{\Delta\nu_{2ndZeeman}}{\nu_0} = 8\times\left(\frac{\nu_{1-1}}{\nu_0}\right)^2, \quad (1)$$

where ν_0 is the clock transition frequency (9192631770Hz). And, the frequency offset due to the magnetic inhomogeneity along the atomic path is given by

$$\frac{\Delta\nu_{offset}}{\nu_0} = 427.45\times10^8\cdot\frac{\delta B^2}{\nu_0}, \quad (2)$$

with δB is the variance of the magnetic field with the unit of Tesla. We measured a map of the time-averaged magnetic field <B> over atomic path. The C-field of CsF1 is typically 125nT and the variance in time is 0.4nT. The second-order Zeeman shift is calculated from (1). From (2), the offset due to the magnetic inhomogeneity is of the order of 10^{-19}, which is practically negligible. The uncertainty of the second-order Zeeman shift is dominated by the temporal instability of B. In NICT-CsF1, the temporal variation of the monitored transition frequency over one month is less than 0.5Hz, leading to an uncertainty of less than 1×10^{-16}.

Bias	Type B Uncertainty
+72.5	<0.1

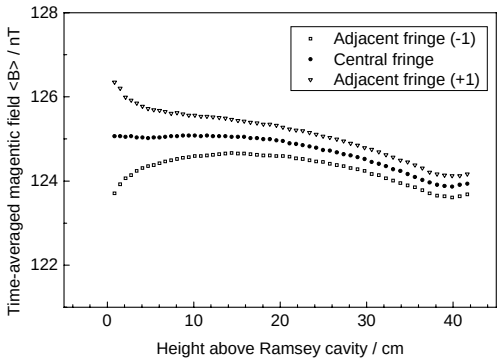

Fig. 1 Map of the time-averaged magnetic field over the atomic path with different launching heights.

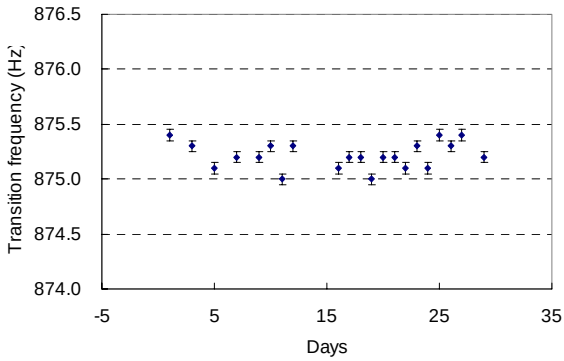

Fig. 2 Tracking of the central frequency of the (F = 4, m_F = 1) – (F = 3, m_F = 1) transition.

B. Collision Shift

The collisional frequency shift is given by $\Delta\nu_{col} = nv\lambda(v)$, where n is the atomic density, v is the relative velocity, and λ is the collisional cross section. The shift $\Delta\nu_{col}$ is evaluated by extrapolating to zero density. Only the intensity of the microwave, that pumps the atoms to the (F=3, m_F=0) state through the selection cavity, is controlled to vary the atomic number density not to change the initial atomic cloud size. Linearity between the frequency shift and the atomic number density has been confirmed, as shown in the figure below. The slope coefficient $\alpha(=v\lambda(v))$ is calculated as -8.2 with a standard deviation of 1.7 in the unit used in Fig.3. From this result, we estimate the frequency shift due to the cold collisions with 20% uncertainty. This large uncertainty is attributed to the fact that the number of the launched atoms is not counted directly but estimated indirectly from the signal intensity of the fluorescence induced by the probe laser.

During the measurement campaign, we do not use this historical slope constant for the zero-density extrapolation. CsF1 is operated alternatively with two different atomic number densities (high and low densities) to correct for the collisional shift at each measurement. The collision shift for 10 or 15 days period is between -8×10^{-15} and -10×10^{-15}. The averaged value is -9×10^{-15} and then the associated uncertainty of 1.8×10^{-15} in NICT-CsF1.

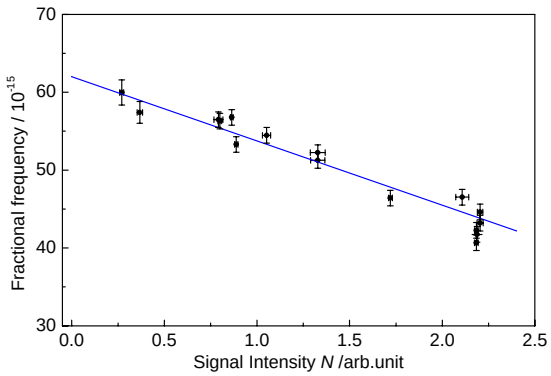

Fig. 3 The fractional frequency difference between NICT-CsF1 and the hydrogen maser as a function of the number of detected atoms.

Bias	Type B Uncertainty
-9.0	1.8

* typical value

C. Black Body Radiation Shift

The frequency shift due to a black body radiation is given by [2]

$$\frac{\Delta \nu_{BBR}}{\nu_0} = -1.711 \times 10^{-14} \left(\frac{T}{300} \right)^4 \times \left[1 + 0.014 \left(\frac{T}{300} \right)^2 \right].$$

The room, where CsF1 is settled, is well temperature controlled at 297 ± 0.2 K. Therefore, the temperature of the drift tube is very stable during the practical operation, even CsF1 itself is not temperature-controlled. Typically, CsF1 is operated at 298 K in equilibrium (a bit higher than the room temperature because of the heats from the devices), which generates a bias of -16.9×10^{-15}. Considering the thermal gradient and the thermal conductivity, we estimate an uncertainty of 0.4×10^{-15} corresponding to ± 2 K.

Bias	Type B Uncertainty
-16.9	0.4

D. Gravitational Red Shift

The gravitational red shift is given by

$$\frac{\Delta \nu_{gravi}}{\nu_0} = \frac{gh}{c^2} \quad .$$

The height of CsF1 is measured as 114.7m in the GRS80 reference flame, which corresponds to 76.6m above the geoid surface. Here we used Japanese geoid model 'GSIGEO2000'[3]. The frequency bias due to the gravity potential is calculated to be 8.4×10^{-15}. Considering lunar and solar tidal displacement of the Earth's crust, we estimate the uncertainty in this shift to be below 1×10^{-16}.

Bias	Type B Uncertainty
+8.4	<0.1

E. Microwave-Power Dependence Shift

Microwave-related shifts are evaluated by high power microwave test (changing the microwave field amplitude from $\pi/2$ to $9\pi/2$ (odd multiplies of $\pi/2$)). An evaluation of the frequency shift associated with the microwave is not simple because many systematic effects, for example, microwave purity, microwave leakage, distributed cavity phase, are convoluted in this shift[4,5]. It is, however, considered that the microwave power dependent shift is classified into two types as follows;

- a term linear dependent on the microwave power
- an oscillating term dependent on the microwave amplitude

By the least square fitting with two contributions, the microwave power dependent shift to due to several effects at the amplitude of $\pi/2$ is estimated to be -0.7×10^{-15} with a standard deviation of

0.2×10^{-15}. Considering that the measurement points are not so many, from the aspect of freedom degree of the fitting, we make a modest estimation of an uncertainty of 0.3×10^{-15}.

Bias	Type B Uncertainty
-0.7	0.3

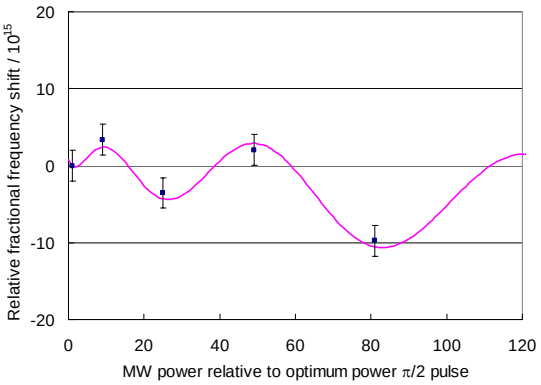

Fig. 4 Measurement of the frequency shift related to the microwave as a function of the microwave power fed to the Ramsey cavity.

F. Uncorrected Frequency Shift

On the following effects, the biases themselves are considered as negligible compared to the measurement precision. So we set the biases to zero. The uncertainties are estimated as the maximum of the possible frequency shift due to the effects.

Cavity pulling shift The resonance frequency of the microwave cavity in CsF1 was well-adjusted to the clock transition in advance. It is not needed to tune the frequency by temperature control. The offset frequency to the clock transition is measured to be less than 700 kHz in the vacuum chamber. We estimate a possible cavity pulling shift is below 1×10^{-16}.

Rabi- and Ramsey–pulling shift In CsF1, it is found that the total number of all $m_F \neq 0$ components is reduced to 10 % of that of $m_F = 0$ components. From the population difference and the frequency offsets of $m_F \neq 0$ transitions, the Rabi pulling shift is calculated to be less than 1×10^{-16}. Though the $\Delta m_F = \pm1$ transitions exist at the offset frequency of ± 450 Hz, the signal intensities of those transition are only 3% of that of the clock transition with more than 90% symmetry. We estimate a possible frequency shift due to the Ramsey-pulling to be less than 1×10^{-16}.

Spectral impurities The phase noise of the low frequency (50 Hz) around the carrier frequency (9.192GHz) of the synthesizer is 90 dB below the carrier. From the theoretical estimation, the possible frequency shift due to the spectral purity is estimated to be much less than 1×10^{-16}.

Light shift All laser beams are blocked by five mechanical shutters during the Ramsey time. The uncertainty of the light shift are estimated to be less than 1×10^{-16}.

Distributed cavity phase shift By numerical calculation using electromagnetic field simulator, the maximum phase variation is estimated to be 7×10^{-7} rad. It is revealed that the phase variance becomes significant when there is a non-zero phase difference between microwaves at two feedings. In NICT-CsF1, by optimizing the phase difference between two feedings, the phase

difference is kept smaller than $\pi/15$, corresponding that the phase variance is 1×10^{-5} rad. Conservatively, the uncertainty of the distributed cavity phase shift is estimated to be 3×10^{-16}. Actually the budget is smaller than this estimation, thanks to the broadening of the atomic cloud.

Majorana transitions The drastic change of the magnetic direction on the atomic path causes a m_F -changing transition, called Majorana transition. The probability of Majorana transition is roughly estimated by $P_{maj} \approx \left(\delta_{mag} V / \Delta_{0-1}\right)^2$, where δ_{mag} is the gradient of the magnetic direction, V is the velocity of atoms (<4.7 m/s), and $\Delta_{0\text{-}1}$ is the transition frequency of $\Delta F = 0$, $\Delta m_F = \pm 1$ transition (450 Hz in NICT-CsF1). The magnetic gradient in CsF1 satisfying the adiabatic condition, the Majorana transition probability is negligibly zero. Even if the Majorana transitions occur, the shift due to the Majorana transition is estimated in the same way as the evaluation of the Ramsey pulling shift. The uncertainty of less than 1×10^{-16} is estimated.

Background gas A high vacuum below 2×10^{-7} Pa has been achieved by using two ion pumps and two non-evaporable getter (NEG) pumps in CsF1. The possible maximum frequency shift, hence the uncertainty, due to the background gas is estimate as below 3×10^{-16}.

Bias	Combined Type B Uncertainty
0	0.4

Table.1. Summary of the systematic frequency biases and their uncertainty budgets of NICT-CsF1.

Physical Effect	Bias	Uncertainty
2nd Zeeman	72.5	<0.1
Collision*	-9.0	1.8
Blackbody Radiation	-16.9	0.4
Gravity Potential	8.4	0.1
MW-PW dependence	-0.7	0.3
Cavity Pulling	0.0	<0.1
Rabi Pulling	0.0	<0.1
Ramsey Pulling	0.0	<0.1
Spectral impurities	0.0	<0.1
Light Shift	0.0	<0.1
Distributed cavity phase	0.0	0.3
Majorana	0.0	<0.1
Background Gas	0.0	0.3

Total (Type B)	*1.9

units are fractional frequency in 10^{-15}
*Typical value

3. Frequency Measurement of NICT-CsF1

In CsF1, the interrogated microwave frequency is locked to the narrow Ramsey resonance by the frequency modulation locking method, in which the microwave is toggled between f_0 - $\Delta\nu/2$ and $f_0 + \Delta\nu/2$, where f_0 is the microwave central frequency and $\Delta\nu$ is the linewidth of the Ramsey fringe, at each cycle. Using the result of one cycle, the microwave frequency f_0 is controlled by steering the output frequency of the synthesizer so that the signal intensities at the two toggled frequencies should be equal. The series of the frequency f_0 are recorded as the frequency realized by CsF1 against the hydrogen maser. At present, the data of our hydrogen maser is not reported to the BIPM. The frequency difference between the hydrogen maser and UTC(NICT) is obtained from time comparison of 1pps signal by a time-interval counter. Combining two differences, the frequency difference between NICT-CsF1 and UTC(NICT) is obtained.

During campaigns, CsF1 is operated at two different atomic number densities in the alternative mode to correct for the collisional shift. The bias of the collisional shift is calculated using 1 day (exactly 85800 seconds) averaging data everyday. The transition frequency of (F=4, m_F =1) – (F=3, m_F =1) transition is tracked for 10 minutes everyday to check the unexpected variation of the magnetic field. The other corrected biases are checked before and after the campaign. Finally, all biases-corrected value is obtained by averaging 10 or 15 sets of 1 day averages.

4. Statistic (Type A) Uncertainty

The frequency stability of CsF1 is typically $4\times10^{-13}/\tau^{1/2}$. Suppose the FM white noise covers over the campaign period, the statistic uncertainty for 10 days or 15 days period becomes the order of 10^{-16}. However, it is difficult to prove it because of the drift of the hydrogen maser. In CsF1, it has been confirmed that the flicker noise floor is no higher than 1.0×10^{-15} by the alternative operation, free from the instability of the reference. From this result, we estimate the Type A uncertainty to be 1.0×10^{-15} conservatively.

5. Uncertainties of Link

The uncertainty $u_{\mathrm{link/lab}}$ of the link to the local time scale, UTC(NICT) is given by a quadratic sum of the uncertainties associated with the frequency transfer between CsF1 and UTC(NICT), and the additional uncertainty due to the dead time during the evaluation campaign. As for the former, the uncertainties come from a measurement accuracy of time-interval counter and link cable fluctuation. There effects are estimated as 3×10^{-16} at most. As for the latter, in this time (four campaigns), the dead time is kept below 2%, which introduces the uncertainty of less than 1×10^{-16}. We evaluate the combined uncertainty associated with the link to be 3×10^{-16}.

The uncertainty in the link of a frequency transfer to TAI is calculated based on the recommendation from the Working Group on Primary Frequency Standards [6]. In our case, the uncertainty $u_{\mathrm{link/TAI}}$ is estimated to be 0.9×10^{-15} (for 15 days period), and 1.2×10^{-15} (for 10 days period).

Reference

[1] Kumagai M, Ito H, Kajita M, and Hosokawa M, *Proc. 2006 Asia-Pacific Workshop on Time and Frequency*, 77-83
[2] Wynands R and Weyers S 2005 Metrologia 42 S64-S79
[3] Nakagawa H, Wada K, Kikkawa T, Shimo H, Andou H, Kuroishi Y, Hatanaka Y, Shigematsu H, Tanaka K, Fukuda Y 2003, *Bulletin of the Geographical Survey Institute* 49, 1
[4] Jefferts S R, Shirley J H, Ashby N, Burt E A, Dick G J 2005 IEEE Trans. Ultraso. Feroel. Freq. Cont. 12 2314-2321
[5] Weyers S, Schröder R, Wynands R *2006 Proc. Euro. Freq. Time Forum*, 173-180
[6] Parker T, Report to the 17th Session of the CCTF, CCTF/06-13, 2006.

Appendix

We calculated the frequency difference between NICT-CsF1 and TAI to check the validity as the primary frequency standard. One month later after the evaluation campaign, the time differences TAI-UTC(NICT) every 5 days are published in Circular T. Using these values from Circular T, we calculated the frequency difference between UTC(NICT) and TAI. The resulting fractional frequency of CsF1 against TAI during several evaluation campaigns are shown in Table.2 and Figure. These results were in good agreement with the BIPM estimation of the duration of the TAI scale interval within the stated uncertainties.

During the 15-days period MJD54079-54094, NICT-CsF1 was operated simultaneously with PTB fountain clock PTB-CSF1 for remote comparison. Each atomic fountain was running referred to each hydrogen maser at each institute. The frequency difference between the hydrogen masers at NICT and PTB was measured directly by the Two-Way Satellite Time and Frequency Transfer (TWSTFT) link between NICT and PTB established in 2005. As a result, NICT-CsF1 and PTB-CSF1 showed a good agreement within the total uncertainty of 2.8×10^{-15}. Detail discussion will be presented elsewhere.

Table.2 Summary of frequency evaluations performed by NICT-CsF1.

Interval	CsF1-UTC(NICT)	TAI-UTC(NICT)	CsF1 - TAI	PFS - TAI *
54014-54029	+0.2	-1.5	+1.7 (2.9)	+3.0 (0.6)
54029-54039	+1.9	-1.2	+3.1 (3.2)	+3.0 (0.6)
54039-54049	-1.4	-1.7	+0.3 (2.3)	+1.7 (0.7)
54079-54094	+3.6	-0.6	+4.2 (2.3)	+1.4 (0.5)

units are fractional frequency in 10^{-15}
total uncertainty is in parentheses
* frequency difference between primary frequency standard and TAI estimated by BIPM

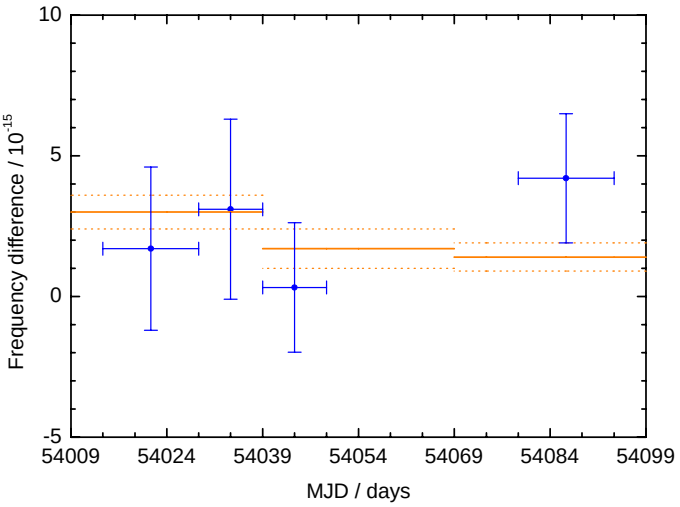

Fig. 5 Frequency difference between NICT-CsF1 and TAI during several campaigns. Solid lines and dotted lines show the frequency differences between primary frequency standard and TAI, and uncertainty ranges, respectively, published in *Circular T*.

Table.3 Direct comparison of NICT-CsF1 with PTB-CSF1 via TWSTFT

	Frequency difference	Uncertainty
PTB-CSF1 – H5	+91.0	1.5
H5 – HM8 (TWSTFT)	-95.0	0.7
NICT-CsF1 – HM8	-2.7	2.2
PTB-CSF1- NICT-CsF1	-1.3	2.8

units are fractional frequency in 10^{-15}
Interval: 54079-54094 (15 days)

Table.4 One-day averages of a campaign (MJD54079-54094)

	CsF1-HM				UTC(NICT)-HM	UTC(NICT)-HM	CsF1-UTC(NICT)
	Hz	x10^-15	x10^-15		x10^-6 (sec)	x10^-15	x10^-15
MJD	Measured frequency	Collision-corrected	All-biases-corrected		time difference at 0:00 UTC	frequency difference	frequency difference
54079	54.9	62.1	-1.2		3.22174	-5.4	4.2
54080	57.8	64.6	1.2		3.22127	0.8	0.4
54081	54.5	51.2	-12.1		3.22134	-0.6	-11.5
54082	52.0	49.2	-14.1		3.22129	-3.1	-11.0
54083	53.5	62.5	-0.8		3.22102	3.5	-4.2
54084	51.8	57.0	-6.3		3.22132	2.8	-9.1
54085	52.9	58.7	-4.6		3.22156	-5.2	0.6
54086	49.2	58.5	-4.8		3.22111	-11.8	7.0
54087	49.3	63.5	0.3		3.22009	-7.8	8.0
54088	52.1	66.7	3.3		3.21942	-16.6	19.8
54089	48.4	57.5	-5.8		3.21799	-11.3	5.5
54090	47.0	62.9	-0.4		3.21701	-11.2	10.8
54091	54.1	67.5	4.3		3.21604	-10.9	15.1
54092	51.5	62.3	-1.0		3.21510	-9.5	8.5
54093	52.6	65.2	1.9		3.21428	-8.8	10.7
54094					3.21352		
	52.1	60.6	-2.7			-6.3	3.6

Collision shift (average): -8.5
2^{nd} Zeeman shift (average): +72.5
Blackbody radiation shift: -16.9
Gravitational red shift: +8.4
Microwave power dependence shift: -0.7
(in the unit of 10^{-15})